

Electrical Resistivity Anisotropy in Fracture Delineation and Characterization: A Case Study of Iwaro-Ayepe Area, Southwestern Nigeria.

C.C. Okpoli (Ph.D. in view)* and O. Igwe, BSc.

Department of Geology, Adekunle Ajasin University, Akungba-Akoko, P.M.B. 001 Ondo State, Nigeria.

E-mail: okpolicyril@gmail.com*

ABSTRACT

The study of electrical resistivity anisotropy in rocks has become important in increasing the accuracy of geological mapping using electrical resistivity survey. The study area, Iwaro-Ayepe in Akoko, southwestern Nigeria, has been surveyed using electrical resistivity soundings in delineation and characterization of the subsurface fracture.

The geological survey showed that the area comprises of granite-gneiss, grey-gneiss and granite. A rose diagram was also produced from values obtained during the geological exercise.

The geophysical survey was carried out in five locations, azimuthal resistivity soundings (ARS) were carried out at each location making a total of twenty (ARS) points. The data obtained were then subjected to various forms of interpretations which includes; computer iterated curves, radial plots and graph of degree of fracture. The resistivity curves comprise of three layer curve types and this includes H, K, Q, and A curve types. The fracture system according to the geological survey (rose diagram) and the ARS, indicates the presence of a localized fracture system which shows mainly NE-SW, NW-SE, E-W trends and very good degree of fracture in location 2, 3, and 4 which is well spread throughout the electrode spacing.

The subsurface fracture characterization is well localized and has directional properties as shown by the geological and geophysical results.

(Keywords: Azimuthal Resistivity Sounding, AZR, geological mapping, subsurface fracture, radial plots, characterization)

INTRODUCTION

The presence of aligned vertical features and vertical to subvertical thin beds causes Anisotropic behavior and inhomogeneity's in rocks. Observed changes in apparent resistivity with azimuth are typically interpreted to indicate fracture anisotropy.

There has been growing need and interest in anisotropy to locate, characterize and identify the directional properties of fractured rock mass in the subsurface. Electrical anisotropy has not been extensively utilized despite of the relevance of electrical technique for detecting fluid filled fracture. This need exist for methods to characterize these fractures economically, quantitatively, and non-invasively and to relate these fractures to their fluid flow properties. For instance, a fractured rock mass has a preferential direction for bulk fluid flow along the major fracture directions.

A relatively inexpensive way to characterize a fractured rock remotely and on a larger volume is by using geophysics, for example resistivity technique. Information about fracture orientation, intensity of porosity and permeability obtained non-invasively is particularly useful to an earth scientist (Boadu et al., 2005).

In field conditions clean fracture and fault planes manifest themselves on geoelectrical sounding curves as cusps marking lateral inhomogeneity (Zohdy et al., 1974). The cusps become more pronounced as the angle of inclination of the fracture approaches 90° . When groundwater flow in shallow depths is to be traced, radial electrode configuration exhibits maximum infiltration potential in the direction of fluid flow (Ogilvy, 1970; Mamah and Ekine, 1989; Sauk and Zabik, 1972).

Observed changes in apparent resistivity with azimuth are typically interpreted to show the presence of fracture anisotropy. Azimuthal resistivity involving different electrode configurations have been used successively to characterize fracture bedrock (Lane et al., 1995; Leonard-Mayer, 1984; Taylor and Fleming, 1988 Clinton et.al, 1984).

The occurrence of groundwater resources in crystalline basement terrain depends immensely on the development of secondary porosity as well as permeability arising from weathering and fracturing of parent rocks and also to great extent on the fracture patterns (Carruthers, 1984). Groundwater in crystalline basement terrain occurs under three principal (Bannerman and Ayibotele, 1984). First, the fractured poorly decomposed or fresh rock overlain by a relatively deep zone of well decomposed rock; secondly, the fractured rocks; and finally, the fractured veins existing in otherwise non water-bearing regolith. (Wright, 1992; Olayinka and Olorunfemi, 1992; Olorunfemi and Fasuyi, 1993). The basement aquifers are often limited in extent vertically and laterally (Satpathy and Kanugo, 1976).

Discontinuous nature of the basement aquifers system necessitates detailed knowledge of the subsurface geology, its weathering and structural disposition through hydrogeological, geological and geophysical investigation. Therefore, groundwater development in crystalline basement terrain is preceded by detailed hydrogeophysical investigations.

LOCATION AND PHYSIOGRAPHY OF THE STUDY AREA

The area under study is located in Akoko in Ondo state, southwestern Nigeria. It is located between longitude $7^{\circ} 30' E$ and $7^{\circ} 25' E$ and latitude $5^{\circ} 45' N$ and $5^{\circ} 50' N$ (Figure 1). Geologically, the area is situated on the Basement Complex of Nigeria which marks about 50% of the total area of Nigeria. The rocks underlying the area are the Migmatite-Gneiss Complex (MGC) rocks (Oyawoye, 1965).

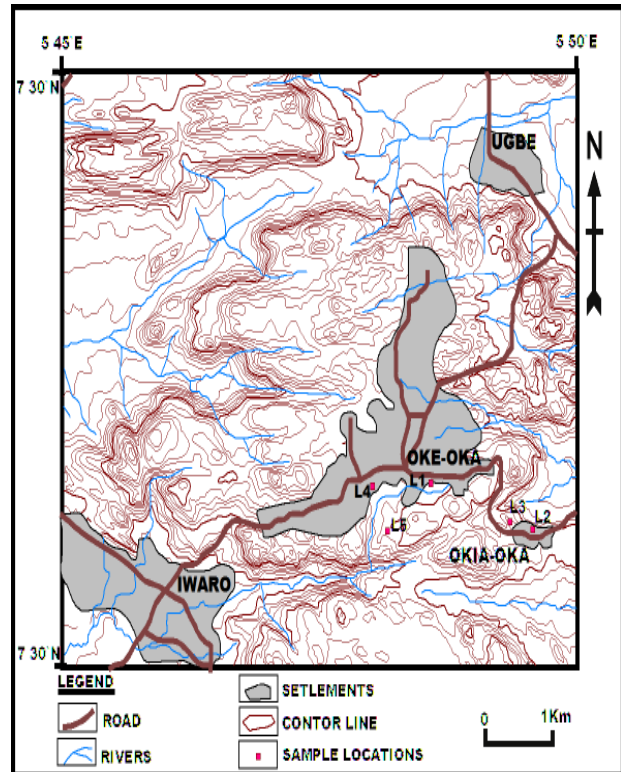


Figure 1: Topographical Map of Study Area.
Source: Extracted from topographical map sheet 265 Owo North-West Ondo State

Geology of the Study Area

Iwaro-Ayeye area lies within the Basement Complex terrain of Nigeria. The Nigerian Precambrian basement rocks are loosely categorized into four main lithologic units. They are: The ancient Gneiss- migmatite complex with ages ranging from mainly Liberian (2800Ma) to Pan African (600 Ma); older dates (>3000 Ma) have lately been obtained from some of the areas. This is also known as Shamrian Orogeny.

The area under study is underlain by migmatite gneiss basement complex (Rahamman, 1973). During the mapping exercise three different rock types were encountered, they are:

- Grey gneiss
- Granite gneiss
- Granite

Grey Gneiss: They commonly occur as hills, series of boundary exposures and low lying exposures. They contain segregation of light and dark silicate minerals, giving them a banded appearance which consists of alternating bands of light feldspar rich zones and dark layers. The light color of the rock is rich in felsic minerals such as feldspar and quartz, while the darker colors are rich in mafic minerals such as mica and hornblende. The gneiss has undergone regional metamorphism and has inferred contact with granite and magmatite.

Granite Gneiss: The granite gneiss occurs mostly as flat or low lying exposures. They are light to dark grey in color with medium grain in size. They consist of lineations as fabrics on the surface. Minerals such as biotite, quartz, feldspar are present. The dominant minerals are mafic minerals and the minor ones are felsic minerals with alternating light and dark mineral bands.

Granites: They are widely distributed in the study area; they occur mostly as hills and flat lying exposures with scanty boundary exposures. The granite has porphyritic texture and the phenocryst is invariably sized. The minerals present include biotite, muscovites, hornblende, alkali feldspar and quartz.

METHODOLOGY

A detailed geological mapping was carried out in the study area to map the trends of the strike and dip directions. Grapher 6 software was used to interpret the structural patterns and their directional properties.

We selected five locations in the study area to be mapped, with each location comprising of four VES soundings. At each of these locations, Radial Vertical Electrical Sounding (RVES) was carried out along four directions; N/S, E/W, NE/SW, NW/SE were distributed to cover the three main rock types in the area so as to observe the correlation between the measured structural directions and the plotted anisotropy polygon directions. The maximum spread of AB/2 in this area is 100 m. It is known that in any formation which is anisotropic due to the presence of fractures, the apparent resistivity (ρ_t) measured normal to its strike direction is greater than apparent resistivity (ρ_s) measured along the

strike direction, when Schlumberger or Wenner array is used but contrary when crossed square array method is employed (Lane et al., 1995).

Field trials show that the anisotropic analysis not only accounts for the major part of the observed orientational variations in resistance, but also yields sounding curves of resistivity, anisotropy and strike, which vary systematically with electrode spacing. The apparent resistivity was measured along four different azimuths N-S, NE-SW, NW-SE and E-W for a given AB/2 separations and were plotted along their corresponding azimuths. Lines of the resistivity of the same value along different azimuths were joined together, thus resulting in a polygon. A set of such polygons obtained corresponding to different AB/2 separations is known as a polar diagram or anisotropy polygon. For an isotropic homogeneous formation, this polygon will assume a circular shape. Any deviation from a circle to an ellipse is indicative of anisotropic nature of the formation (Mallik et al., 1983). The major or longest axis of the ellipse, which can fit any of such anisotropic polygons, gives the strike direction of the fracture. Coefficient of anisotropy is a useful parameter of an anisotropic medium and can be defined as:

$$\lambda_a = \sqrt{\rho_{at}/\rho_{as}}$$

The co-efficient of apparent anisotropy (λ_a) (designated here as the degree of fracturing) is calculated from each anisotropy ellipse (fitted through each polygon).

The rose diagram shows the general fracture trend of the area is mainly N-E, S-E, and E. The calculated λ_a values are then plotted against the corresponding AB/2 separations. The behavior of rock fracturing at various depth equivalents to different AB/2 separations can thus be understood qualitatively from the variation of λ_a (Habberjam, 1975). From the 60 RVES survey carried out, the apparent resistivity anisotropy polygon was plotted and coefficient of anisotropy was calculated for each station, using the methods of Habberjam (1972,1975, 1979), Lane et al. (1995), Mallik et al. (1983), Annor et al. (1990), and Okurumeh and Olayinka (1998). The data obtained were plotted against the electrode spacing on bilogarithm coordinates and a preliminary interpretation was carried out using partial curves matching involving two-layer master curves and the appropriate auxiliary charts. The

use of WINRESIST was a final stage in quantitative data interpretation.

RESULTS AND DISCUSSION

The qualitative and quantitative interpretation of geological and geophysical data namely the strike direction, foliation planes, joint direction and radial vertical electrical sounding, respectively, area equally useful in correlating surface and subsurface fractures. The combined interpretation of geological field trials and azimuthal resistivity sounding data had clearly brought out the subsurface fracture orientation. The result of the RVES data for the study area were plotted and interpreted.

Table 1 shows the selected values of the radial plots, their locations, electrode spacing and values.

Figure 2 shows a rose diagram obtained using Grapher 8 software to plot the strike directions and foliation planes observed in the basement rock during the geological mapping of the study area. The result of the rose diagram, displays NE, E and SE directions prominently.

The anisotropy polygons were gotten by selecting specific distances (AB/2) for each location was 25, 32, 40 and 65m. The various locations comprises of VES1-4, 5-8, 9-12,13-16 and 17-20 as shown in the table below, and these were regarded as locations 1,2,3,4, and 5, respectively.

The radial plot is used to describe fracture directions at specific positions. The interpreted fracture directions for the selected plots are summarized in table 2 the major or longest axis of the ellipse, which can fit any of such anisotropic polygons, gives the strike direction of the fracture. The values of coefficient of anisotropy calculated for each location is presented in table, and was used to plot the graph of degree of fracture this was used to detect the degree of fracture at depth with respect to electrode spacing AB/2 for each location. The interpretations are as follows:

Location 1: This location consists of azimuthal resistivity sounding 1-4. The degree of fracture is well striking at electrode spacing (AB/2m) 10, 40, 50 and 65m with corresponding degree of fracturing as 1.5, 2.6, 2.5 and 2.5.

Location 2: This consists of azimuthal resistivity sounding of 5-8. The degree of fracturing is well striking throughout the electrode spacing. Where the electrode spacing (AB/2m) is 10 and 25 the intensity of fracture is 1.7 and 1.9, respectively, and where (AB/2m) is 45 and 65, the corresponding intensity of fracture is 1.6 and 2.4.

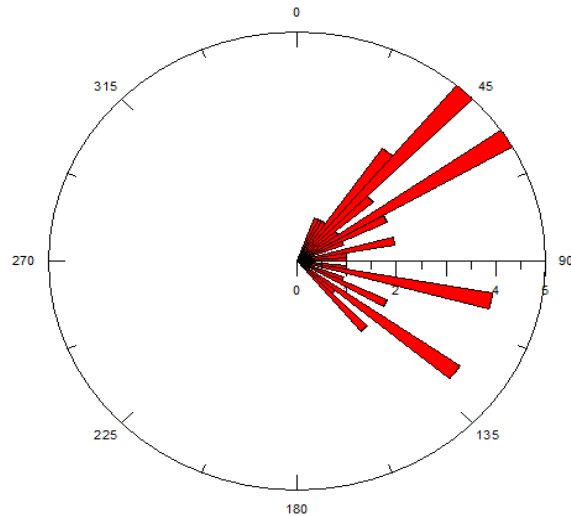


Figure 2: The Rose Diagram of the Strike and Foliation Planes of Iwaro-akoko Study Area.

Table 1: Selected Values for Radial Plots.

| Locations | Distances | Values | | | |
|-----------|-----------|--------|------|------|------|
| 1 | 25 | 147 | 346 | 234 | 186 |
| | 32 | 166 | 474 | 317 | 209 |
| | 40 | 67 | 618 | 330 | 788 |
| | 65 | 338 | 541 | 854 | 507 |
| 2 | 25 | 549 | 432 | 813 | 227 |
| | 32 | 491 | 564 | 325 | 448 |
| | 40 | 706 | 788 | 1347 | 1294 |
| | 65 | 1272 | 840 | 661 | 497 |
| 3 | 25 | 565 | 382 | 661 | 590 |
| | 32 | 612 | 834 | 910 | 1104 |
| | 40 | 276 | 1018 | 836 | 1367 |
| | 65 | 939 | 1581 | 1993 | 2648 |
| 4 | 25 | 248 | 363 | 316 | 353 |
| | 32 | 260 | 372 | 422 | 425 |
| | 40 | 175 | 605 | 699 | 462 |
| | 65 | 400 | 450 | 480 | 836 |
| 5 | 25 | 442 | 55 | 105 | 68 |
| | 32 | 635 | 125 | 127 | 276 |
| | 40 | 901 | 189 | 334 | 1324 |
| | 65 | 187 | 230 | 129 | 4799 |

Location 3: This consists of azimuthal resistivity sounding 9-12. The fracture is well striking at some points where (AB/2m) is 12m and 35 with degree of fracture as 1.6 and 2.4, respectively.

Location 4: This consists of azimuthal resistivity sounding 13-16. The fracture is well striking at some points where (AB/2m) is 6, 8 and 35 with corresponding degree of fracture as 2.3, 1.8 and 2.0.

Location 5: This consists of azimuthal resistivity sounding 17-20. The degree of fracture is well defined at point where electrode spacing (AB/2m) is 65 and with corresponding degree of fracture as 6.5.

Table 3 and 4 were used to plot the scatter diagram and its interpretations respectively; as it applies to the degree of subsurface fractures. Figure 3-9 displays the diverse radial plots at selected electrode spacing where the trends/directional properties of the subsurface fractures. Figure 3 and 4 at location 1 show the orientations of fracture at location 1 show the orientations of subsurface fracture at electrode spacing of 25 and 32 and it is aligned at NE-SW direction respectively.

Location 2, we observe in figure 5 the presence of highly fractured rock at depth corresponding to AB/2 of 40m and its orientation in NE-SW. In figure 6 and 7 the resistivity polygons are oriented along W-E and NW-SE directions and it corresponds to electrode spacing of 40m and 65m respectively. In location 5, there are two different sets of resistivity polygons (Figures 8 and 9) at 25m and 65m electrode spacing and it is found orienting along N-S and NW-SE directions, respectively.

In Figure 10, location1 the degree of fracturing increases with increasing electrode spacing. The fracture is more pronounced at the point where AB/2 equals 40m to 60m. Figure 11 shows a scatter diagram for location indicating that the degree of fracture is intense throughout the electrode spacing especially at AB/2 equals 10m to 65m.

We observe that in Figure 12, that the intensity of fracture is prominent at AB/2 equals 12m, 15m and 45m. Figure 13, shows a scatter diagram

whose degree of fracturing is intense at electrode spacing of 6m,8m and 35m while Figure 14, location 5, we observe a prominent degree of fracture at electrode spacing of 65m.

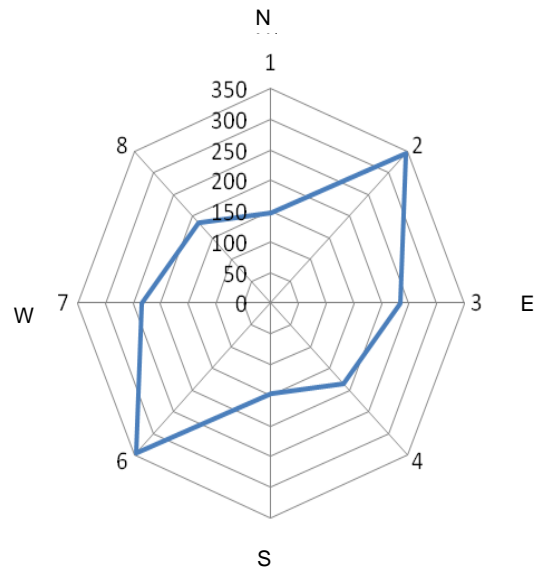


Figure 3: Radial plot at AB/2=25m in Location 1.

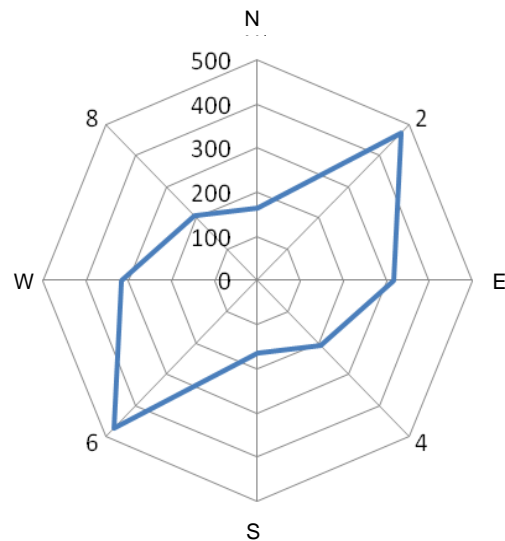


Figure 4: Radial plot at AB/2=32m in Location 1.

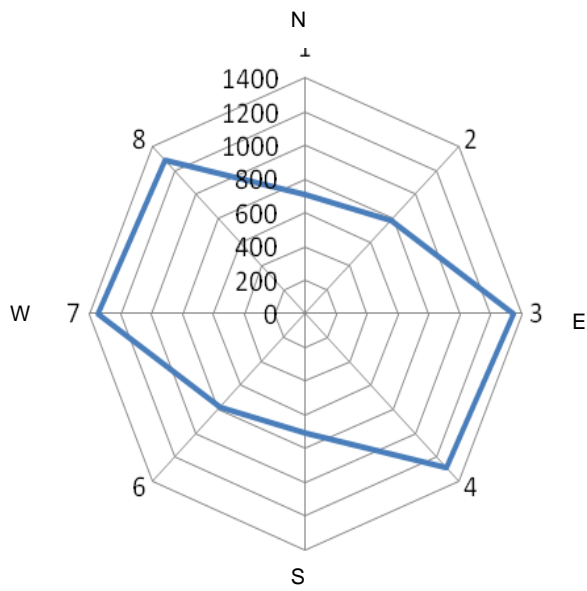


Figure 5: Radial plot at $AB/2=40m$ in Location 2.

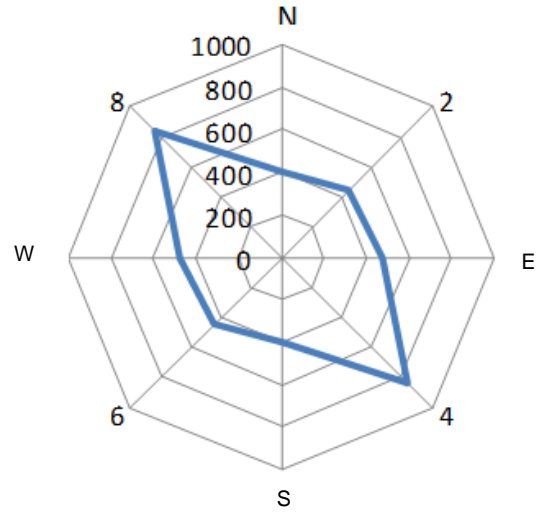


Figure 7: Radial plot at $AB/2=40m$ in Location 4.

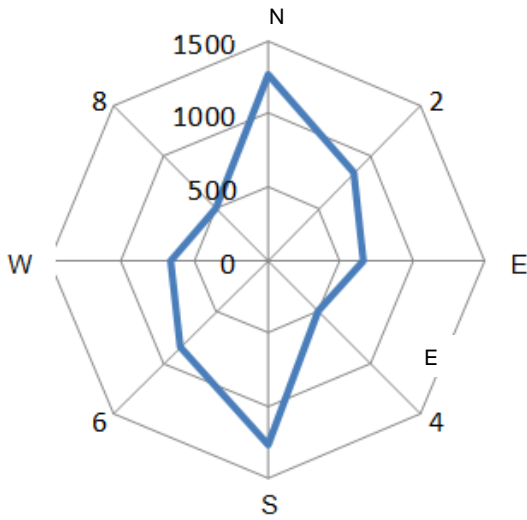


Figure 6: Radial plot at $AB/2=40m$ in Location 4.

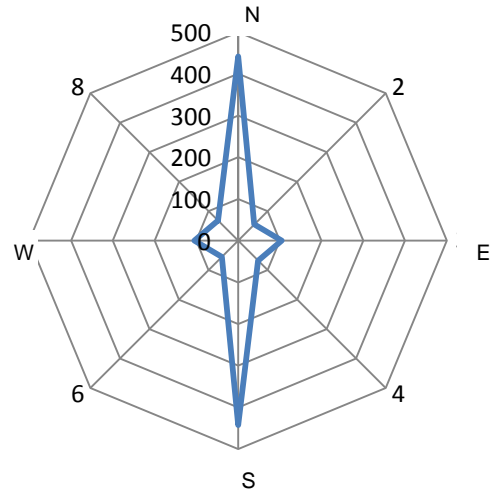


Figure 8: Radial plot at $AB/2=25m$ in Location 5.

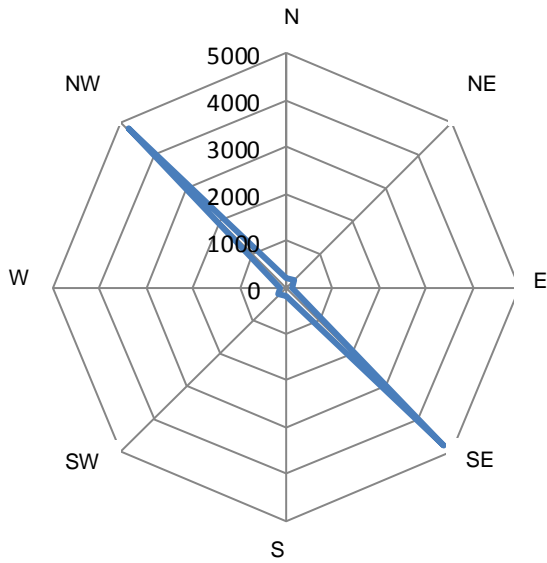


Figure 9: Radial plot at AB/2=25m in Location 5.

Table 2: Interpretation of Selected Radial Plots.

| Location | Selected AB/2(m) | Interpretation of fracture direction |
|----------|------------------|--------------------------------------|
| 1 | 25 32 | NE/SW NE/SW |
| 2 | 40 65 | NE/SW N/S |
| 3 | 40 65 | NW/SE NW/SE |
| 4 | 40 65 | W/E NW/SE |
| 5 | 25 65 | N/S NW/SE |

Table 3: Values used for Scatter Diagram.

| Distance AB/2 | Location 1 | Location 2 | Location 3 | Location 4 | Location 5 |
|---------------|------------|------------|------------|------------|------------|
| 1 | 1.3 | 1.0 | 1.1 | 1.2 | 1.2 |
| 2 | 1.1 | 1.1 | 1.0 | 1.1 | 1.1 |
| 3 | 1.1 | 1.1 | 1.1 | 1.0 | 1.2 |
| 4 | 1.0 | 1.3 | 1.1 | 2.1 | 1.2 |
| 6 | 1.0 | 1.6 | 1.2 | 1.5 | 1.3 |
| 6 | 1.0 | 1.7 | 1.1 | 1.8 | 1.2 |
| 8 | 1.5 | 1.4 | 1.2 | 1.3 | 1.3 |
| 12 | 1.2 | 1.4 | 1.0 | 1.3 | 1.4 |
| 15 | 1.3 | 1.2 | 1.6 | 1.1 | 1.3 |
| 15 | 1.1 | 1.6 | 1.3 | 1.0 | 1.5 |
| 25 | 1.6 | 1.9 | 1.3 | 1.2 | 2.5 |
| 32 | 1.7 | 1.3 | 1.4 | 1.3 | 2.3 |
| 40 | 1.6 | 1.4 | 2.2 | 1.9 | 2.6 |
| 40 | 2.6 | 1.6 | 1.3 | 1.2 | 2.7 |
| 65 | 2.5 | 1.6 | 1.6 | 1.5 | 6.1 |

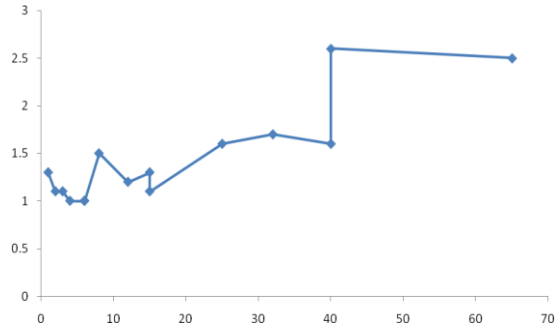


Figure 10: Scatter Diagram for Location 1.

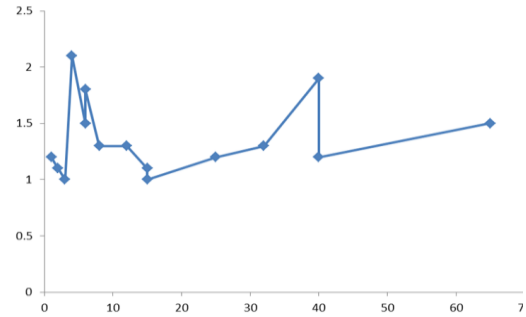


Figure 13: Scatter Diagram for Location 4.

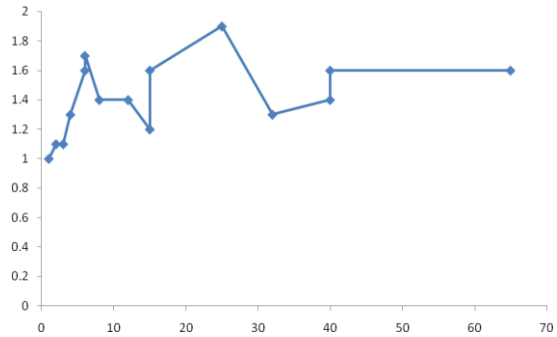


Figure 11: Scatter Diagram for Location 2.

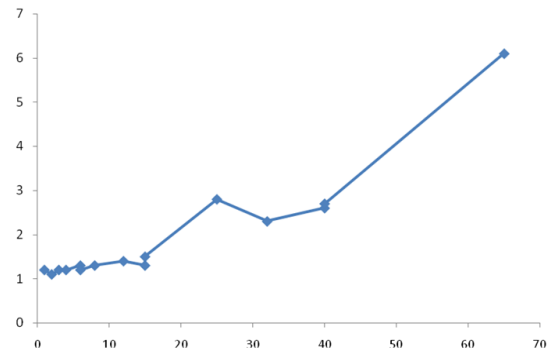


Figure 14: Scatter Diagram for Location 5.

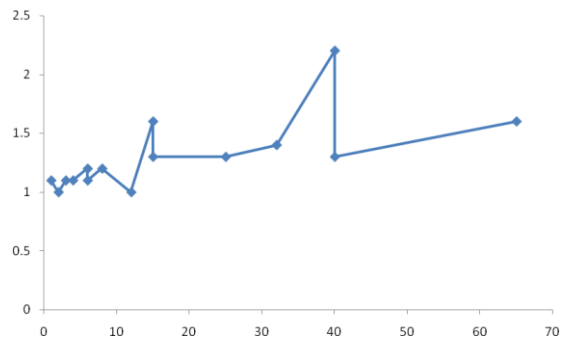


Figure 12: Scatter Diagram for Location 3.

Table 4: Interpretation of Scatter Diagram.

| Locations | Intensity of Fracture with Electrode Spacing |
|-----------|--|
| 1 | In location 1, fracture increases with increasing electrode spacing. The fracture is more at the point where $AB/2=40-65m$. |
| 2 | Fracture is intense throughout the electrode spacing from $AB/2=10-65m$. |
| 3 | Intense at some points where $AB/2=12-15m$ and $45m$. |
| 4 | Intense at points where $AB/2=6,8$ and 35 . |
| 5 | The fracture is intense at the point where $AB/2=65m$. |

CONCLUSION

The study area, Iwaro-ayepe, southwestern Nigeria was investigated using RVES techniques. This technique was used to delineate and characterize subsurface fracture of the area. Both approach area able to identify and correlate the orientations of the surface and subsurface and depth extent of fractures.

Initially, the geological mapping helped in delineating the trends of the Precambrian crystalline basement surface fractures, followed by azimuthal resistivity sounding method, which clearly characterize the subsurface fracture system. This was achieved by the use of radial vertical electrode sounding. The salient features of the combined effect of these two methods are that the fracture system according to the geological survey (rose diagram) and the azimuthal resistivity sounding (ARS) indicates the presence of a localized fracture system which shows mainly NE-SW, NW-SE, E-W trends and very good degree of fracture in location 2, 3, and 4 which is well spread throughout the electrode spacing.

Fracture orientations obtained from the geophysical azimuthal soundings agrees with those obtained from geological mapping. Anisotropy polygons and scatter diagrams were also generated and interpreted to describe fracture direction and degree of fracture with respect to depth respectively. The relatively higher values of anisotropy and fracture porosity and the relatively lower values of specific surface area imply that the fractured mass in these areas is likely to be intensely fractured and more permeable.

REFERENCES

1. Annor, A.E, P.I. Olasehinde, and P.C. Pal. 1990. "Basement Fracture Patterns in the Control of Water Channels, An example from Central Nigeria". *J. Min. Geol.* 26(1):5-11.
2. Bannerman, R.R. and N.B. Ayibotele. 1984. "Some Critical Issues with Monitoring Crystalline Rock Aquifers for Groundwater Management in Rural Area. Challenges in Africa Hydrology and Water Resources". IAHS publication.No.144, pp 47-56.
3. Boadu, F.K, J. Gyamfi, and E. Owusu. 2005. "Determining Subsurface Characteristics from Azimuthal Resistivity Surveys: A Case Study at Nsawam, Ghana". *Geophysics.* 70(5):B35-B45.
4. Bauchanan, I.J.1983. International Water Technology Conference and Exposition (AUGA EXPO' 83). Acapulco, Mexico
5. Caruthers, R.M. 1984. "Reviews of Geophysical Techniques for Groundwater Exploration in Crystalline Basement Terrain". *British Geological Survey Report.* No. RGRG85/3.
6. Clinton, J.P. and A.K. Smith Carrington. 1984. "Characteristics of Weathered Basement Aquifers in Malawi in Relation to Rural Water Supply". *IAHS Publications,* No. 144 Pp 57-72.
7. Habberjam, G.M. 1972. The Effect of Anisotropy on Square Array Resistivity Measurements". *Geophysical Prospecting.* 20:249-266.
8. Habberjam, G.M, and G.E. Watkins. 1967. "The Use of Square Configuration in Resistivity Prospecting". *Geophysical Prospecting.*15: 221-235.
9. Lane, J.W., Jr., F.P. Haeni, and W.M. Wetson. 1995. "Use of Square-Array Direct-Current Resistivity Method to Detect Fractures in Crystalline Bedrock in New Hampshire. Groundwater". *U.S. Geological Survey Bulletin.* 33(3): 476-485.
10. Leonard-Mayer, P.J. 1984a. "A Surface Resistivity for Measuring Hydrogeologic Characteristics of Jointed Formations". US. Bureau of Mines report of Investigations 8901.
11. Leonard-Mayer, P.J. 1984b. "Development and Use of Azimuthal Resistivity Surveys for Jointed Formations". *Proceedings of the National Water Well Association.* U.S. Environmental Protection Agency Conference on Surface and Borehole methods in Groundwater Investigations. San Antonio, TX. D.M. Nielsen and Mary Curl. Eds. Worthington, OH: National Water Well Association. 52-91.
12. Lewis M.R and F.P. Haeni. 1987. "The Use of Surface Geophysical Techniques to Detect Fractures in Bedrock". *An Annotated Bibliography of U.S Geophysical Survey Circular.* 987:14.
13. Mallik, S.B, D.C. Bhattacharya, and S.K. Nag. 1983. "Behavior of Fractures in Hard Rocks-a Study by Surface Geology and Radial VES Method". *Geoexploration.* 21(3):181-189.
14. Mammah, L.I. and A.S. Ekine.1989. "Electrical Resistivity Anisotropy and Tectonism in Basal Nsukka Formation". *Journal of Mining and Geology.* 25 (1 and 2):121-128.

15. McCurry, P. 1976. "The Geology of Precambrian to Lower Paleozoic Rocks of Northern Nigeria. A Review". In: Kogbe C.A.(ed). Elizabeth Publ. Co.: Ibadan, Nigeria. 15-38.
16. Ogilvy, A.A. 1970. "Geophysical Prospecting for Groundwater in the Soviet Union in Mining and Groundwater Geophysics". Economic Geologic Report No.26:536-543. Canada.
17. Olayinka, A.I. 1996. "Non-Uniqueness in the Interpretation of Bedrock Resistivity from Sounding Curves and its Hydrological Implications". *Water Resour. J. NAH*, 7(1&2): 55-60.
18. Olayinka, A.I and M.O. Olorunfemi. 1992. "Determination of Geoelectrical Characteristics in Okene Area and Implications for Borehole Siting". *Journal of Mining and Geology*. 28(2):403-412.
19. Olorunfemi, M.O. and S.A. Fasuyi. 1993. "Aquifer Types and Geoelectric/Hydrogeologic Characteristics of Part of Central Basement Terrain of Nigeria (Niger State)". *J. Africa Earth Sci.* 16(3): 309-317.
20. Okurumeh, O.K. and A.I. Olayinka. 1998. "Electrical Anisotropy of Crystalline Basement Rocks around Okeho, Southwestern Nigeria: Implications in Geologic Mapping and Groundwater Investigation". *Water Resour. J. NAH*. 9:41-50.
21. Oyawoye, M.O. 1964. "The Geology of Nigerian Basement Complex-A Survey of Our Present Knowledge of Them". *Jour. Of Min. Geo. and Intell.* 1(2):87-193.
22. Rahaman, M.A. 1973. "Review of the Basement Geology of Southwestern Nigeria". In: *Geology of Nigeria*. Kobe, C.A (ed). 2nd ed. Rockview Publishers: Jos, Nigeria.
23. Satpatty, B.N, and B.N. Kanugo. 1976. "Groundwater Exploration in Hard Rock Terrain, A Case Study". *Geophysical Prospecting*. 24(4):725 – 736.
24. Sauck, W.A. and S.M. Zabik. 1992. "Azimuthal Resistivity Techniques and the Directional Variations of Hydraulic Conductivity in Glacial Sediments". In: *SAGEEP '92*, Society of Engineering and Mineral Exploration Geophysicists: Golden, CO. 197-222.
25. Wright, E.P. 1992. "The Hydrogeology and Crystalline Basement Aquifers in Africa". In: Wright, E.P. and Burgess, W.G. (eds). *Hydrogeology of Crystalline basement Aquifers in Africa*. Geological Society of London Special Publication. No. 66, pp 713-728.
26. Zohdy, A.A. 1974. "Application of Surface Geophysics to Groundwater Investigation". *Techniques of Water Resources Investigations of the US Geological Survey, Book 2*, pp. 5-6. USGS: Washington, D.C.

ABOUT THE AUTHORS

Cyril C. Okpoli, is with the Department of Geology and Applied Geophysics, PMB 001, Akungba- Akoko, Ondo State, Nigeria and has research interests in environmental geophysics and well modeling.

O. Igwe, is with the Department of Geology and Applied Geophysics, PMB 001, Akungba-AKoko, Ondo State, Nigeria and has research interests in environmental geophysics.

SUGGESTED CITATION

Okopoli, C.C. and O. Igwe. 2013. "Electrical Resistivity Anisotropy in Fracture Delineation and Characterization: A Case Study of Iwaro-Ayepe Area, Southwestern Nigeria". *Pacific Journal of Science and Technology*. 14(2):488-497.